Dermal Sensory Regenerative Peripheral Nerve Interface for Reestablishing Sensory Nerve Feedback in Peripheral Afferents in the Rat

Sando, Ian C.; Adidharma, Widya; Nedic, Andrej; Ursu, Daniel C.; Mays, Elizabeth A.; Hu, Yaxi; Kubiak, Carrie A.; Sugg, Kristoffer B.; Kung, Theodore A.; Cederna, Paul S.

Published in:
Plastic and Reconstructive Surgery

DOI:
10.1097/PRS.0000000000010086

Dermal Sensory Regenerative Peripheral Nerve Interface for Reestablishing Sensory Nerve Feedback in Peripheral Afferents in the Rat

Ian C. Sando, MD[1]
Widya Adidharma, MD[2]
Andrej Nedic, MD[2]
Daniel C. Ursu, PhD[2]
Elizabeth A. Mays, PhD[2]
Yaxi Hu, MD[3]
Carrie A. Kubiak, MD[2]
Kristoffer B. Sugg, MD, PhD[2]
Theodore A. Kung, MD[2]
Paul S. Cederna, MD[2]
Gregory J. Gerling, PhD[4]
Stephen W. P. Kemp, PhD[2]
Melanie G. Urbanchek, PhD[2]

Carmel, IN; Ann Arbor, MI; Groningen, the Netherlands; and Charlottesville, VA

Background: Without meaningful, intuitive sensory feedback, even the most advanced myoelectric devices require significant cognitive demand to control. The dermal sensory regenerative peripheral nerve interface (DS-RPNI) is a biological interface designed to establish high-fidelity sensory feedback from prosthetic limbs.

Methods: DS-RPNIs were constructed in rats by securing fascicles of residual sensory peripheral nerves into autologous dermal grafts, with the objectives of confirming regeneration of sensory afferents within DS-RPNIs and establishing the reliability of afferent neural response generation with either mechanical or electrical stimulation.

Results: Two months after implantation, DS-RPNIs were healthy and displayed well-vascularized dermis with organized axonal collaterals throughout and no evidence of neuroma. Electrophysiologic signals were recorded proximal from DS-RPNI's sural nerve in response to both mechanical and electrical stimuli and compared with (1) full-thickness skin, (2) deepithelialized skin, and (3) transected sural nerves without DS-RPNI. Mechanical indentation of DS-RPNIs evoked compound sensory nerve action potentials (CSNAPs) that were like those evoked during indentation of full-thickness skin. CSNAP firing rates and waveform amplitudes increased in a graded fashion with increased mechanical indentation. Electrical stimuli delivered to DS-RPNIs reliably elicited CSNAPs at low current thresholds, and CSNAPs gradually increased in amplitude with increasing stimulation current.

Conclusions: These findings suggest that afferent nerve fibers successfully reinnervate DS-RPNIs, and that graded stimuli applied to DS-RPNIs produce proximal sensory afferent responses similar to those evoked from normal skin. This confirmation of graded afferent signal transduction through DS-RPNI neural interfaces validate DS-RPNI's potential role of facilitating sensation in human-machine interfacing. *(Plast. Reconstr. Surg.* 151: 804e, 2023.)

Clinical Relevance Statement: The DS-RPNI is a novel biotic-abiotic neural interface that allows for transduction of sensory stimuli into neural signals. It is expected to advance the restoration of natural sensation and development of sensorimotor control in prosthetics.

From [1]Plastic and Reconstructive Surgery, Ascension St. Vincent Medical Group; the [2]Section of Plastic Surgery, University of Michigan Health System; [3]University Medical Center Groningen; and [4]Systems and Engineering, University of Virginia.
Received for publication December 2, 2020; accepted April 26, 2022.
The first two authors are co–first authors.
The last two authors are co–senior authors.
Presented at Plastic Surgery: The Meeting 2015, the Annual Meeting of the American Society of Plastic Surgeons, in Boston, Massachusetts, October 16 through 20, 2015.

DOI: 10.1097/PRS.0000000000010086

Disclosure statements are at the end of this article, following the correspondence information.

This work was supported by THE PLASTIC SURGERY FOUNDATION.

Related digital media are available in the full-text version of the article on www.PRSJournal.com.

Persons with amputations cannot currently feel what they touch with their prostheses. For individuals with upper extremity amputation, sensory feedback is critical to providing more naturalistic control of prosthetic devices.[1–5] Recent advances in myoelectric prosthetic technology[6–8] bring us closer to providing sensory function to prostheses. However, current neural interfaces cannot reliably convey sensor-derived information into meaningful, intuitive sensory feedback. The ideal sensory interface should limit damage to afferent nerves, demonstrate biological stability over time, offer natural perceptions of sensation, be modality matched, and be somatotopically matched (perceived in the same location as on the missing limb). Unfortunately, current interfaces lack one or more of these essential qualities.[1–5,7,8]

To date, the most promising techniques for restoring sensory feedback for persons with amputations use the peripheral nervous system. Recent work focused on a variety of peripheral nerve interfaces developed to bridge the gap between bioelectric and mechanical signals.[9–12] These techniques use both noninvasive and invasive techniques and include extraneural cuff electrodes,[13–15] flexible nerve plates,[16] intrafascicular electrodes,[17–19] and penetrating electrodes.[20–22] However, these interface techniques have limitations regarding nerve specificity, tissue injury, axonal degeneration, scar formation, and lack of long-term stability.

Targeted sensory reinnervation (TSR) is an interface method in which residual mixed nerves in the upper extremity are surgically rerouted to the chest or transhumeral residual limb and coapted to either (1) mixed nerves with subsequent reinnervation of the skin overlying the reinnervated muscle,[23–25] or (2) sensory nerves in the chest or proximal upper extremity.[26,27] Touching the reinnervated skin evokes sensations perceived as originating from the missing limb. However, TSR is limited by nerve coaptation size mismatch, lack of selectivity, instability, and variable somatotopic representation.[6,25–27]

To overcome these limitations of current neural interfaces, we developed the dermal sensory regenerative peripheral nerve interface (DS-RPNI). The DS-RPNI is a modification of our regenerative peripheral nerve interface (RPNI), which consists of a free muscle graft secured around the distal end of transected nerves.[12,28] Here, RPNI muscle grafts are reinnervated by regenerating axons from the transected nerve, and are capable of amplifying independent efferent motor action potentials to allow real-time prosthetic finger control.[11,29] The DS-RPNI consists of small deepithelialized skin grafts secured around fascicles of residual sensory nerves. They are placed subcutaneously and are quickly reinnervated by the residual nerve sensory afferents. Different sensory nerves can be attached to independent deepithelialized skin grafts to create a series of DS-RPNIs, allowing sensory feedback from many distinct and spatially segregated locations.

We envision human DS-RPNIs being constructed (1) within the surface skin for stimulation through surface electrodes or (2) deep for stimulation through implanted electrodes. We deepithelialize the skin to avoid the formation of keratin cysts while in a subcutaneous location and because the epithelium would potentially be a barrier to rapid DS-RPNI revascularization. We hypothesized that (1) DS-RPNIs would become revascularized over time; (2) sensory afferents would regenerate and reinnervate the dermal grafts; (3) graded mechanical stimuli applied to DS-RPNIs would evoke compound sensory nerve action potentials (CSNAPs), similar to normally innervated skin; and (4) pulsed electrical stimuli applied to DS-RPNIs would elicit graded CSNAP output with waveform amplitudes that are comparable to those evoked when graded mechanical stimuli are applied to normal skin.

MATERIALS AND METHODS

Study Design

Forty male 3-month-old F344 rats (Harlan Laboratories, Inc., Haslett, MI) were assigned to receive either endpoint mechanical or electrical stimulation. [**See Figure, Supplemental Digital Content 1**, which shows study design, example images, and testing equipment diagrams. (*Above*) Study design: 40 hindlimbs were assigned to mechanical stimulation, and then randomized to one of four experimental groups: control full-thickness skin (*CFS*), control deepithelialized skin (*CDS*), control transected nerve (*CN*), or dermal skin interface (*DSI*). (*Center, left*) Right foot positioned in the testing mold with ceramic indenting tip (3 mm) positioned over sural nerve–innervated glabrous skin. (*Below, left*) Lateral view of right foot showing full-thickness skin. (*Below, center*) Lateral view of right foot showing control deepithelialized skin. (*Center, right*) Mechanical indenter (*d*, sural nerve; *e*, tibial nerve; *f*, accelerometer; *h*, ground electrode). *Scale bar* = 0.5 cm, ***http://links.lww.com/PRS/F772***. **See Figure, Supplemental Digital Content 2**, which shows (*above*) study design: 40 hindlimbs were assigned to electrical stimulation, and then randomized to one of four experimental groups: control full-thickness skin (*CFS*), control deepithelialized skin (*CDS*), control transected

nerve (*CN*), or dermal skin interface (*DSI*). (*Below, left*) Left skin flap isolated in a silicone-lined dish with stimulating electrodes positioned deep and superficial on a glabrous skin flap (same for control full-thickness skin and control deepithelialized skin). (*Below, center*) View of dissected left sural nerve with stimulating electrodes place deep and superficial (same for control nerve and dermal sensory interface). (*Below, right*) *a*, *b*, positive and negative stimulating electrodes; *c*, pulse generator; *d*, silicone dish/mold; *e*, control full-thickness, control deepithelialized skin, control nerve, or dermal sensory interface; *f*, sural nerve; *g*, tibial nerve; *h*, *j*, *k*, positive and negative recording electrodes; *i*, ground electrode; *l*, amplifier. *Scale bar* = 0.5 cm, ***http://links.lww.com/PRS/F773***.] The hindlimbs were then randomized to one of four experimental groups: (1) control full-thickness skin (CFS); (2) control deepithelialized skin (CDS); (3) control nerve with no dermal skin interface (CN); and (4) DS-RPNI. Ten additional rats were included for tissue donation. All procedures were approved by the Institutional Animal Care and Use Committee and were conducted in accordance with the *Guide for the Care and Use of Laboratory Animals*.[30] For all surgical and endpoint procedures, rats were deeply anesthetized. Rats received subcutaneous carprofen for analgesia before anesthesia with isoflurane.

Survival Operations

Glabrous skin on the hind feet of 10 anesthetized donor rats was deepithelialized until pinpoint, dermal bleeding was observed using a rotary dermabrasion tool (Dremel, Racine, WI). Skin grafts measuring 0.5 × 1.0 cm were harvested from each foot, defatted, and kept moist for later implantation. An incision was made on the dorsal aspect of the lower hindlimb and the gastrocnemius muscle was separated longitudinally. The sural nerve was carefully dissected free. For each CN hindlimb, the sural nerve was traced to the lateral malleolus, where it was cauterized and segmentally excised, creating an approximately 8-mm nerve gap. Single DS-RPNIs were surgically constructed in designated DS-RPNI recipient hindlimbs. (**See Figure, Supplemental Digital Content 3**, which shows DS-RPNI fabrication in a rat. (*Left*) Deepithelialized glabrous skin graft is positioned under the transected end of the sural nerve. (*Right*) The graft is folded cephalically to enclose the sural nerve and is secured with suture, ***http://links.lww.com/PRS/F774***.) The sural nerve was first transected midway between the knee and ankle. A deepithelialized skin graft was placed deep to the sural nerve with the deep layer of the dermis in contact with the residual end of the transected sural nerve. A 1.0-mm segment of sural epineurium was removed, and fascicles were splayed across the center of the skin graft. The distal portion of the graft was folded cephalically to enclose the splayed end of the nerve. The skin graft was then secured to itself and to the epineurium.

Endpoint Testing

CFS and CDS Group Preparations

In vivo endpoint testing was performed at 5 months. Rats were anesthetized; left and right hindlimbs were evaluated sequentially. Sural nerve was carefully exposed through a skin incision, and a bipolar cuff electrode with 30-gauge platinum leads (Grass Technologies, Warwick, RI) was connected to a differential amplifier and electrophysiologic recording system (RZ2; Tucker-Davis Technologies, Alachua, FL). This recording electrode was placed on the sural nerve approximately 3.2 cm proximal to the stimulation site and distal to the sciatic nerve bifurcation. The recording electrode and its positioning were the same for both mechanical and electrical stimulation protocols.

Sites undergoing mechanical stimulation were positioned in a custom mold and secured with hydrocolloid to maintain normal tension. The entire hindfoot was stabilized for CFS and CDS glabrous skin mechanical stimulation. To accommodate CN and DS-RPNI mechanical stimulation, the residual sural nerve or the DS-RPNI was dissected free and rotated away from the hindlimb before stabilization in a mold. A mechanical indenter then applied graded compression. (**See Document, Supplemental Digital Content 4**, which shows the mechanical stimulation protocol, ***http://links.lww.com/PRS/F775***.)

For hindlimb sites undergoing electrical stimulation, neurocutaneous flaps (CFS and CDS groups) were elevated to electrically isolate the sural nerve receptive field and avoid electromyographic signal interference. A stimulating pad electrode (E363-76H-1-SPL; Plastics One, Inc., Roanoke, VA) was secured to the external surface of the flap and a reference electrode was placed deep to the flap. Electrical stimulations were delivered and recordings were evaluated using a custom multichannel acquisitions system (TDT RZ2; Tucker-Davis). Signals were analyzed offline in MATLAB (The MathWorks, Inc., Natick, MA). Three dependent variables were recorded: (1) absolute threshold, (2) discrimination sensitivity, and (3) repeatability. (**See Document,**

Supplemental Digital Content 5, which shows the electrical stimulation protocol, ***http://links.lww.com/PRS/F776***.)

Once endpoint testing was complete, tissues were harvested and evaluated for angiogenesis, tissue viability, scar tissue formation, nerve regeneration, construct reinnervation, and neuroma formation. Rats were euthanized.

Histologic Analysis

At the conclusion of endpoint evaluations, experimental tissues were harvested and preserved in 10% formalin. Tissues were stained with hematoxylin and eosin and Masson trichrome to evaluate dermal integrity, presence of inflammation, and revascularization. Antibodies against neurofilament were used to assess axonal regeneration and nerve fiber distribution within dermal tissues.

Statistical Analysis

Data were analyzed separately for experimental groups evaluated by the mechanical stimulation modality and for those evaluated by the electrical stimulation modality. The central tendency of data for each dependent variable was statistically compared across experimental groups using a one-way analysis of variance. When the analysis of variance indicated a significant difference existed for the main effect, multiple comparison tests were performed using a Bonferroni correction. Calculations were performed using IBM SPSS Version 21.0 (IBM Corp., Armonk, NY), with a value of $P < 0.05$ considered statistically significant.

RESULTS

Histologic Analysis

At endpoint evaluations, all DS-RPNIs demonstrated robust revascularization with minimal scar encapsulation and no keratin cyst formations. In each CN hindlimb, small terminal neuromas developed at the residual end of each sural nerve. Tissues were well perfused, with capillary ingrowth extending to the central portion of DS-RPNIs. Neuromas were not observed in DS-RPNIs. [**See Figure, Supplemental Digital Content 6**, which shows the DS-RPNI. (*Left, above*) Illustration of a dermal sensory interface (DS-RPNI) consisting of deepithelialized skin grafts reinnervated by sensory (sural) nerve. (*Left, below*) DS-RPNI in vivo 2 months after fabrication showing revascularization and minimal scar tissue. (*Second from left*) Terminal sural nerve neuroma that developed in a control animal 2 months after the nerve was transected. (*Second from right, above* and *below*) Hematoxylin and eosin and trichrome immunohistochemistry show angiogenesis throughout the DS-RPNI with multiple capillaries (*arrowheads*) interspersed among healthy connective tissue. (*Right*) Neurofilament staining (*red*) demonstrates regenerated sural nerve axons (*arrows*) in the superficial DS-RPNI dermis. Magnification in immunohistochemical stains, 40×, ***http://links.lww.com/PRS/F777***.]

Mechanical Stimulation

Mechanical stimuli applied to experimental tissues evoked CSNAPs that were recorded from the proximal sural nerve. Supplemental Digital Content 7 depicts representative raw sural nerve potential and instantaneous CSNAP firing rates in response to the three levels of indentation on native full-thickness glabrous skin. CSNAP amplitude and firing rates increased with increasing depth of skin indentation. Peak CSNAP amplitude and instantaneous firing rate were approximately 60 μV and 800 Hz, respectively, when skin was displaced to a depth of 3 mm. Compared with periods of static pressure, stimulus (hold phase), amplitudes, and firing rates were higher during periods of moving stimulus (ramp phase) for each level of displacement. [**See Figure, Supplemental Digital Content 7**, which shows sural nerve response to indentation on full-thickness skin. Example recordings made during mechanical displacements of 1 mm (*left*), 2 mm (*center*), and 3 mm (*right*) at constant velocity into native full-thickness glabrous skin. Tracings of recorded potential at proximal sural nerve are shown (*above*) over a 6-second duration. *Green bars* indicate periods of moving stimulus (ramp phase), and *red bars* indicate periods of static pressure stimulus (hold phase). (*Below*) Tracings are instantaneous CSNAP firing rates during mechanical displacement, ***http://links.lww.com/PRS/F778***.]

CSNAP amplitude and firing rates are quantified in Supplemental Digital Content 8. Experimental group CSNAP data are summarized for three levels of displacement during the ramp and hold phases of indentation. Mean CSNAP amplitudes and firing rates were significantly higher for the ramp phase when compared with the hold phase within each group ($P < 0.05$). At 2 mm of tissue displacement, CSNAP firing rates were significantly higher for DS-RPNIs compared with CFS, CDS,

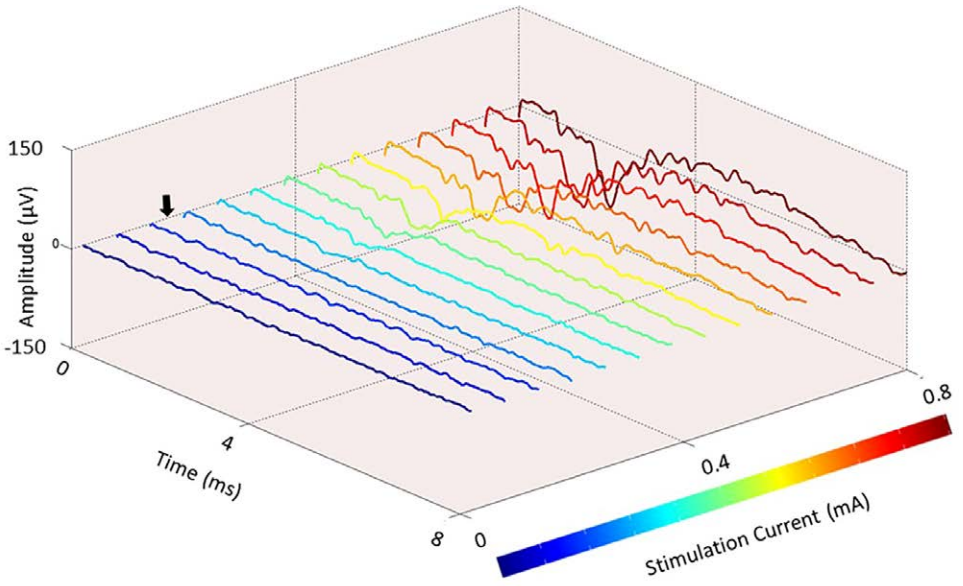

Fig. 1. Electrically evoked CSNAPs from a DS-RPNI. Time-synced CSNAP traces were recorded at the proximal sural nerve during electrical stimulation of a DS-RPNI. *Colored lines* are example sural nerve recordings as stimulation pulse amplitude was varied from 0 to 0.8 mA during delivery of 200 individual pulses. Recording data are shown starting at 0.15 msec to eliminate stimulus artifact. *Violet* indicates subthreshold stimulation amplitude during which no CSNAPs were elicited, and *red* indicates elicitation of CSNAPs as pulse amplitude was increased above threshold current (*light blue*, 0.34 mA). As pulse amplitude increased above threshold, CSNAPs were elicited with increased waveform amplitude.

and CN groups ($P < 0.05$). During both phases of indentation, CSNAP amplitudes and firing rates directly increased in a graded fashion for each group. [**See Figure, Supplemental Digital Content 8**, which shows mechanically evoked CSNAP amplitudes of control and experimental tissues. Mean (*above*) CSNAP amplitude and (*below*) firing rates are shown for (*left*) ramp and (*right*) hold phases of indentation at three displacement depths into full-thickness glabrous skin, deepithelialized glabrous skin, control transected nerve, and DS-RPNIs. For each group, CSNAP amplitudes and firing rates are greater during the ramp phase compared with the hold phase for each level of displacement. Note that DS-RPNIs show a similar increase in firing rate for increased depths of displacement compared with native skin. *Error bars* = SEM. *Horizontal bars* indicate statistical significance, which was set at $P < 0.05$, ***http://links.lww.com/PRS/F779***.]

Electrical Stimulation

Stimulation Current at Absolute Threshold

Independent evoked CSNAP waveforms were reliably detected above a threshold stimulation current. Figure 1 depicts representative time-synced sural nerve potentials recorded from the proximal sural nerve as stimulation pulse amplitude was varied from 0 to 0.8 mA. CSNAP waveforms were detected at threshold stimulation current, with amplitudes increasing thereafter with increases in current. Stimulation currents at absolute threshold are compared between experimental groups in Figure 2. Thresholds were significantly lower for the CN group when compared with DS-RPNI and control skin groups ($P < 0.05$).

Current Response Curve

CSNAP amplitude increased in a similar linear fashion in response to increases in stimulation current for DS-RPNI and control skin groups but not for the CTN group (Fig. 3). Compared with DS-RPNI and control conditions, CSNAP amplitude was more sensitive to changes in current when stimuli were applied directly to control nerve ($P < 0.05$); in other words, each incremental increase in stimulation current generated greater CSNAP amplitude. Application of electrical stimuli produced CSNAP amplitudes similar to those evoked during mechanical stimulation experiments. CSNAP amplitudes (15 to 40 μV) evoked during indentation into native full-thickness skin

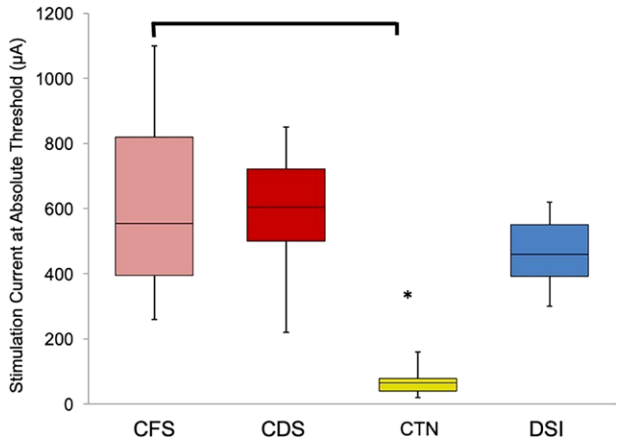

Fig. 2. Stimulation currents for eliciting CSNAPs at absolute threshold. Comparison of threshold stimulation current needed to elicit CSNAPs for full-thickness glabrous skin, deepithelialized glabrous skin, control transected sural nerve (*CTN*), and DS-RPNIs. Box plots indicate first, second (median), and third quartiles, and minimum and maximum values. *Significance compared with control full-thickness skin. Statistical significance was set at $P < 0.001$.

are depicted in Figure 3. These amplitudes were evoked over a narrower range of electrical stimulation currents for the CTN group (0.012 mA) compared with the DS-RPNI group (0.1 mA).

Repeatability of Elicited Response

The percentage CSNAP elicitation and mean CSNAP amplitude during delivery of pulses to experimental group tissues at 10, 20, 50, and 100 Hz are presented in Table 1. At frequencies less than or equal to 100 Hz, electrical stimuli applied on DS-RPNIs reliably evoked CSNAPs over 96% of the time. Pulses delivered at 100 Hz evoked CSNAPs with lower amplitudes than those delivered at lower frequencies, although this difference did not reach statistical significance.

DISCUSSION

Myoelectric prosthetic users rate sensory feedback as one of the most important priorities, and lack of sensory feedback is one of the leading causes of prostheses abandonment.[1,2,31–33] Sensory

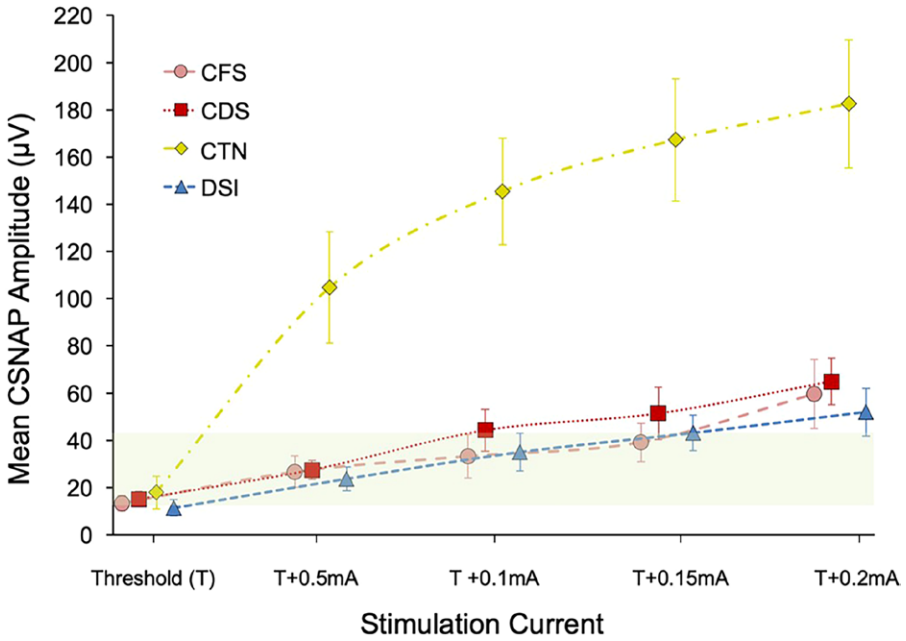

Fig. 3. Electrically evoked CSNAP amplitude for native and experimental tissue. Mean CSNAP amplitude recorded at the proximal sural nerve with differential increase in stimulation current for full-thickness glabrous skin, deepithelialized glabrous skin, control transected nerve, and DS-RPNIs. Stimulation current was incremented at 0.05 mA. CSNAPs were normalized to threshold (*T*) for each trial. In response to increased stimulation current, CSNAP amplitude increases in a similar linear fashion for DS-RPNI and control skin groups but not for the CTN group. CSNAP amplitudes evoked during indention on full-thickness skin are depicted by the *shaded box*. Similar amplitudes were evoked during delivery of pulsed electrical stimulation to DS-RPNIs over a range of 0.1 mA. *Error bars* = SEM.

Table 1. Summary Data by Experimental Group for CSNAP and Peak-to-Peak Voltage Recorded from Sural Nerve during Stimulus Delivery at Different Frequencies[a]

Stimulation Frequency (Hz)	CFS		CDS		CTN		OSI	
	% Elicitation	Vpp (μV)	% Elicitation	Vpp (μV)	% Elicitation	Vpp (μV)	% Elicitation	Vpp (μV)
10	98.6 ± 3.8	32.7 ± 27.4	99.4 ± 1.3	38.6 ± 26.1	99.8 ± 0.6	160.0 ± 92.2	99.6 ± 0.8	31.0 ±14.8
20	98.6 ± 3.1	32.8 ± 29.3	100 ± 0	42.3 ± 30.7	100 ± 0	145.4 ± 71.4	99.4 ± 1.3	33.6 ± 26.5
50	98.4 ± 3.7	28.5 ± 20.7	98.6 ± 4.4	35.6 ± 23.6	99.7 ± 0.9	162.3 ± 99.9	96.8 ± 5.5	30.6 ±19.1
100	97.2 ± 3.9	36.7 ± 20.6	98.0 ± 3.0	30.3 ± 16.2	100 ± 0	150.2 ± 97.3	97.0 ± 5.6	24.2 ± 16.9

Vpp, peak-to-peak voltage.
[a]Stimulation delivery was 100 pulses with constant pulse amplitude of threshold ±0.1 mV. Values are CSNAP elicitation percentage ± SD and CSNAP waveform mean ± SD. Results show that the Vpp values for the DS-RPNI group were not significantly different from either the CFS or CDS group on statistical analysis.

feedback is important for improved control of the prosthetic limb,[4,5,34] sense of embodiment,[34] and reduction of phantom limb pain.[22,35] Although marked advancements in the mechanical and sensing capabilities of the modern prosthetic have been made, restoration of sensory function remains a challenge, largely in part because of the lack of a reliable sensory interface between the prosthetic device and the user.[6] The ideal neural interface should be stable, maintain natural sensation, and support somatotopic- and modality-matched sensory feedback. Here, we show that DS-RPNIs can successfully provide graded sensory feedback by demonstrating that: (1) sensory axons successfully regenerate and reinnervate DS-RPNI dermal grafts without evidence of neuroma formation; (2) patterned electrical stimuli evoke highly reproducible and graded sensory nerve action potentials, comparable to those evoked during mechanical indentation of normal skin; and (3) graded mechanical compression of DS-RPNIs evokes highly reproducible and graded sensory nerve action potentials similar to normal skin.

Many different epineural[34,36–38] and intraneural[4,39–41] electrode configurations have been used to facilitate prosthetic control, with several studies demonstrating improved sensorimotor control and the ability to elicit a range of sensory qualities.[4,5,37,40,42] However, a major disadvantage of interfacing directly with the nerve, particularly with epineural and intraneural designs, are the associated unnatural percepts that are attributable to the inadvertent widespread activation of neighboring bundles of different types of sensory afferents,[3,4,37,43] resulting in sensory feedback that is unnatural and not somatotopically/modality matched.[3–5] Furthermore, interfacing directly with nerves may injure delicate neural tissue and lead to demyelination, axonal degeneration, and scar tissue formation.[44–48] Several studies have reported that this gradual biofouling of electrodes occurs over time, which leads to an increasing need for higher amplitude electrical stimulation to elicit a perceivable sensation.[5,40,41] Although advances in material properties have improved biocompatibility of chronically implanted electrodes,[48,49] electrode-induced neural injury may limit the ability of these intraneural interfaces to elicit tactile sensations long term.[41]

Previously, our group developed the RPNI to create an interface with greater signal specificity and long-term signal stability.[12,28] The muscle graft is reinnervated by the implanted nerve and reliably amplifies independent efferent motor action potentials from the transected motor nerve, which allows upper limb amputees real-time prosthetic finger control.[12,29] Furthermore, RPNIs prevent and treat neuroma pain and phantom limb pain in patients with limb loss.[50,51] Sensory nerves can innervate muscle as evidenced by histologic and functional confirmation of Golgi apparatus and muscle spindle reinnervation by sensory nerves in the "babysitter" technique for sensory nerve protection of denervated skeletal muscle.[52,53] However, a more optimal target for a sensory afferent would be dermal sensory organs. The dermal graft of the DS-RPNI provides a barrier between peripheral afferents and stimulating electrodes, which prevents direct neural injury caused by traumatic electrode implantation, foreign body response, or chronic micromotion. We have demonstrated that the free dermal flap becomes revascularized and remains viable 2 months after fabrication. In addition, we show that axons regenerate into the dermis without evidence of neuroma formation (**see Figure, Supplemental Digital Content 6**, ***http://links.lww.com/PRS/F777***).

The DS-RPNI exploits the advantages of providing sensory feedback using reinnervated skin, but also addresses the limitations that hamper other interfaces. A single DS-RPNI can be created for each sensory nerve, allowing for sensory feedback from as many anatomical locations as desired. Implantation of transected sensory

nerves into DS-RPNIs amplifies the number of independent sites of sensory input, because each DS-RPNI encases only a small sensory nerve or group of sensory fascicles. In addition, as sensory axons reinnervate different territories of the dermal grafts of the DS-RPNI, selective activation of fibers may be possible by delivering electrical stimuli to different locations on the interface using multichannel electrodes. With this approach, it is possible to provide greater specificity of elicited sensations, improved spatial resolution, and more natural sensation by activating different sensory afferents in different areas of the DS-RPNI, thus offering a somatotopically organized interface. This is in contrast to the TSR technique. Although TSR also avoids direct contact with nerves and has been shown to evoke sensation with stimulation of reinnervated skin, the nature of how TSR is constructed results in lack of functional selectivity and variable somatotopic representation. The recipient skin decides both the spatial resolution and how the skin ends up being reinnervated by rerouted nerves, which is inconsistent between patients. In addition, touching adjacent patches on the chest/upper arm does not necessarily correspond to sensations on adjacent parts of the amputated limb, and touching a singular patch may result in the perception of sensations on multiple parts of the amputated limb.[6,23,25,27,54]

In the current study, threshold currents to elicit sensory responses were significantly lower for control nerves compared with DS-RPNIs and native skin. Using longitudinal intrafascicular electrodes to directly activate peripheral afferents, Dhillon et al. showed that tactile sensations are evoked at low current thresholds.[55] However, as stimulus current increases, subjects experienced strong shock-like sensations. We found that incremental increases in CSNAP amplitude were evoked over a broader range of stimulation currents when electrical stimuli were applied to DS-RPNIs as compared with when nerves were directly stimulated. This suggests that by adjusting the stimulation current applied to DS-RPNIs, gradations in sensory feedback may be more precisely modulated than with direct nerve stimulation.

Although sensory recovery of denervated glabrous skin has been described in the clinical setting,[56,57] to our knowledge, this is the first study to demonstrate that mechanical stimulation of neurotized, deepithelialized, glabrous skin grafts elicits graded sensory nerve responses. Results showed that CSNAP responses were unique during ramp and hold phases of mechanical indentation for both normal skin and DS-RPNIs. This suggests that sensory afferents, which have reinnervated DS-RPNIs, are capable of sensing mechanical stimuli and retain their ability to produce differential responses to moving and static stimuli, respectively. This in turn implies that the different mechanoreceptors remain intact within the dermal graft and are likely to be reinnervated by their unique afferent Aβ fibers. Meissner and Pacinian corpuscles are rapidly adapting and respond to onset/offset of tactile stimuli (corresponding to ramp phase), and Merkel cells and Ruffini endings respond to sustained tactile loads (corresponding to hold phase).[7,58] It is possible that implantable actuators in DS-RPNIs could deliver compression forces of differential intensities to evoke graded sensations in patients with limb loss.

We acknowledge certain limitations with our study. First, we have yet to elucidate the mechanisms responsible for the maintenance of nerve health within DS-RPNIs. Although low-threshold mechanoreceptors within dermis are known targets for nerve regeneration,[59,60] these sensory organelles may be compromised during deepithelialization and skin graft thinning, which are essential surgical techniques to ensure graft survival and minimize the chances of epidermal inclusion cyst formation in the DS-RPNIs. Instead, dermal-derived Schwann cells may play a critical role orchestrating nerve regeneration and providing continued trophic support to regenerated axons within DS-RPNIs.[61–64] Future studies aim to characterize the distribution of specific sensory axons within DS-RPNIs and identify potential targets for reinnervation. There is evidence that afferents may be clustered in the nerve based on their submodality,[65–67] and thus, we would predict each DS-RPNI to be modality specific.[68,69]

SUMMARY

Both mechanical and electrical graded sensory stimulation applied to DS-RPNIs reproducibly evoked graded CSNAPs at low thresholds of pressure and current. The attributes of the DS-RPNI—including anatomical specificity of sensation, lack of competition for skin area, avoidance of neuroma formation, conservation of residual nerve tissue, and ability to provide multiple independent sites for sensory input—merit further consideration of the DS-RPNI for providing sensory feedback from prosthetic devices for patients with limb loss.

Stephen W. P. Kemp, PhD
University of Michigan
1150 West Medical Center Drive
Medical Sciences Research Building II, Room A570
Ann Arbor, MI 48109-5456
swpkemp@med.umich.edu
Instagram: umichnml

DISCLOSURE

The authors have no financial interest to declare in relation to the content of this article.

ACKNOWLEDGMENTS

This study was supported by American Foundation for Surgery of the Hand Basic Science grant N018515, a Plastic Surgery Foundation Research Fellowship, the Society for University Surgeons, and Ethicon. The authors thank J. Moon and members of the Muscle Mechanics Laboratory for helpful discussions.

REFERENCES

1. Cordella F, Ciancio AL, Sachetti R, et al. Literature review on needs of upper limb prosthesis users. *Front Neurosci.* 2016;10:1–14.
2. Wijk U, Svensson P, Antfolk C, Carlsson I, Björkman A, Rosén B. Touch on predefined areas on the forearm can be associated with specific fingers: towards a new principle for sensory feedback in hand prostheses. *J Rehabil Med.* 2019;51:209–216.
3. Antfolk C, D'Alonzo M, Rosén B, Lundborg G, Sebelius F, Cipriani C. Sensory feedback in upper limb prosthetics. *Expert Rev Med Devices* 2013;10:45–54.
4. Petrini FM, Valle G, Strauss I, et al. Six-month assessment of a hand prosthesis with intraneural tactile feedback. *Ann Neurol.* 2019;85:137–154.
5. Clemente F, Valle G, Controzzi M, et al. Intraneural sensory feedback restores grip force control and motor coordination while using a prosthetic hand. *J Neural Eng.* 2019;16:026034.
6. Svensson P, Wijk U, Bjorkman A, Antfolk C. A review of invasive and non-invasive sensory feedback in upper limb prostheses. *Expert Rev Med Devices* 2017;14:439–447.
7. Osborn LE, Dragomir A, Betthauser JL, et al. Prosthesis with neuromorphic multilayered e-dermis perceives touch and pain. *Sci Robot.* 2018;3:10.1126/scirobotics.aat3818.
8. Valle G, Mazzoni A, Iberite F, et al. Biomimetic intraneural sensory feedback enhances sensation naturalness, tactile sensitivity, and manual dexterity in a bidirectional prosthesis. *Neuron* 2018;100:37–45.e7.
9. del Valle J, Navarro X. Interfaces with the peripheral nerve for the control of neuroprostheses. *Int Rev Neurobiol.* 2013;109:63–83.
10. Mioton LM, Dumanian GA. Targeted muscle reinnervation and prosthetic rehabilitation after limb loss. *J Surg Oncol.* 2018;118:807–814.
11. Frost CM, Ursu DC, Flattery SM, et al. Regenerative peripheral nerve interfaces for real-time, proportional control of a neuroprosthetic hand. *J Neuroeng Rehabil.* 2018;15:108.
12. Vu PP, Vaskov AK, Irwin ZT, et al. A regenerative peripheral nerve interface allows real-time control of an artificial hand in upper limb amputees. *Sci Transl Med.* 2020;12:eaay2857.
13. Brill NA, Nuafel SN, Polasek K, et al. Evaluation of high-density, multi-contact nerve cuffs for activation of grasp muscles in monkeys. *J Neural Eng.* 2018;15:036003.
14. Song KI, Park SE, Lee S, Kim H, Lee SH, Youn I. Compact optical nerve cuff electrode for simultaneous neural activity monitoring and optogenetic stimulation of peripheral nerves. *Sci Rep.* 2018;8:15630.
15. Song KI, Park SE, Hwang D, Youn I. Compact neural interface using a single multichannel cuff electrode for a functional neuromuscular stimulation system. *Ann Biomed Eng.* 2019;47:754–766.
16. Stieglitz T, Schuettler M, Schneider A, Valderrama E, Navarro X. Noninvasive measurement of torque development in the rat foot: measurement setup and results from stimulation of the sciatic nerve with polyimide-based cuff electrodes. *IEEE Trans Neural Syst Rehabil Eng.* 2003;11:427–437.
17. Zheng X, Zhang J, Chen T, Chen Z. Longitudinally implanted intrafascicular electrodes for stimulating and recording fascicular physioelectrical signals in the sciatic nerve of rabbits. *Microsurgery* 2003;23:268–273.
18. Zhen G, Chen H, Tsai S-Y, Zhang J, Chen T, Jia X. Long-term feasibility and biocompatibility of directly microsurgically implanted intrafascicular electrodes in free roaming rabbits. *J Biomed Mater Res B Appl Biomater.* 2019;107:435–444.
19. Jung R, Abbas JJ, Kuntaegowdanahalli S, Thota AK. Bionic intrafascicular interfaces for recording and stimulating peripheral nerve fibers. *Bioelectron Med (Lond.)* 2018;1:55–69.
20. Urbanchek MG, Wei B, Egeland BM, Abidian MR, Kipke DR, Cederna PS. Microscale electrode implantation during nerve repair: effects on nerve morphology, electromyography, and recovery of muscle contractile function. *Plast Reconstr Surg.* 2011;128:270e–278e.
21. Wendelken S, Page DM, Davis T, et al. Restoration of motor control and proprioceptive and cutaneous sensation in humans with prior upper-limb amputation via multiple Utah Slanted Electrode Arrays (USEAs) implanted in residual peripheral arm nerves. *J Neuroeng Rehabil.* 2017;14:121.
22. Page DM, George JA, Kluger DT, et al. Motor control and sensory feedback enhance prosthesis embodiment and reduce phantom pain after long-term hand amputation. *Front Hum Neurosci.* 2018;12:352.
23. Marasco PD, Schultz AE, Kuiken TA. Sensory capacity of reinnervated skin after redirection of amputated upper limb nerves to the chest. *Brain* 2009;132:1441–1448.
24. Sensinger JW, Schultz AE, Kuiken TA, Org S, Edu A. Examination of force discrimination in human upper limb amputees with reinnervated limb sensation following peripheral nerve transfer. *IEEE Trans Neural Syst Rehabil Eng.* 2009;17:438–444.
25. Kuiken TA, Marasco PD, Lock BA, Harden RN, Dewald JP. Redirection of cutaneous sensation from the hand to the chest skin of human amputees with targeted reinnervation. *Proc Natl Acad Sci USA.* 2007;104:20061–20066.
26. Hebert JS, Chan KM, Dawson MR. Cutaneous sensory outcomes from three transhumeral targeted reinnervation cases. *Prosthet Orthot Int.* 2016;40:303–310.
27. Hebert JS, Olson JL, Morhart MJ, et al. Novel targeted sensory reinnervation technique to restore functional hand sensation after transhumeral amputation. *IEEE Trans Neural Syst Rehabil Eng.* 2014;22:765–773.
28. Svientek SR, Ursu DC, Cederna PS, Kemp SWP. Fabrication of the composite regenerative peripheral nerve interface (C-RPNI) in the adult rat. *J Vis Exp.* 2020;156:10.3791/60841.
29. Kung TA, Langhals NB, Martin DC, Johnson PJ, Cederna PS, Urbanchek MG. Regenerative peripheral nerve interface viability and signal transduction with an implanted electrode. *Plast Reconstr Surg.* 2014;133:1380–1394.
30. Institute for Laboratory Animal Research. *Guide for the Care and Use of Laboratory Animals.* Washington, DC: The National Academies Press; 2010.
31. Biddiss EA, Beaton D, Chau T. Consumer design priorities for upper limb prosthetics. *Disabil Rehabil Assist Technol.* 2007;2:346–357.

32. Schofield JS, Evans KR, Carey JP, Hebert JS. Applications of sensory feedback in motorized upper extremity prosthesis: a review. *Expert Rev Med Devices* 2014;11:499–511.
33. Nghiem BT, Sando IC, Gillespie RB, et al. Providing a sense of touch to prosthetic hands. *Plast Reconstr Surg.* 2015;135:1652–1663.
34. Tyler DJ, Durand DM. Functionally selective peripheral nerve stimulation with a flat interface nerve electrode. *IEEE Trans Neural Syst Rehabil Eng.* 2002;10:294–303.
35. Petrini FM, Bumbasirevic M, Valle G, et al. Sensory feedback restoration in leg amputees improves walking speed, metabolic cost and phantom pain. *Nat Med.* 2019;25:1356–1363.
36. Tan DW, Schiefer MA, Keith MW, Anderson JR, Tyler DJ. Stability and selectivity of a chronic, multi-contact cuff electrode for sensory stimulation in human amputees. *J Neural Eng.* 2015;12:026002.
37. Tan DW, Schiefer MA, Keith MW, Anderson JR, Tyler J, Tyler DT. A neural interface provides long-term stable natural touch perception. *Sci Transl Med.* 2014;6:257ra138.
38. Ortiz-Catalan M, Håkansson B, Brånemark R. An osseointegrated human-machine gateway for long-term sensory feedback and motor control of artificial limbs. *Sci Transl Med.* 2014;6:257re6.
39. Boretius T, Badia J, Pascual-Font A, et al. A transverse intrafascicular multichannel electrode (TIME) to interface with the peripheral nerve. *Biosens Bioelectron.* 2010;26:62–69.
40. Raspopovic S, Capogrosso M, Petrini FM, et al. Restoring natural sensory feedback in real-time bidirectional hand prostheses. *Sci Transl Med.* 2014;6:222ra19.
41. Rossini PM, Micera S, Benvenuto A, et al. Double nerve intraneural interface implant on a human amputee for robotic hand control. *Clin Neurophysiol.* 2010;121:777–783.
42. Oddo CM, Raspopovic S, Artoni F, et al. Intraneural stimulation elicits discrimination of textural features by artificial fingertip in intact and amputee humans. *Elife* 2016;5:e09148.
43. Johansson RS, Flanagan JR. Coding and use of tactile signals from the fingertips in object manipulation tasks. *Nat Rev Neurosci.* 2009;10:345–359.
44. Navarro X, Krueger TB, Lago N, Micera S, Stieglitz T, Dario P. A critical review of interfaces with the peripheral nervous system for the control of neuroprostheses and hybrid bionic systems. *J Peripher Nerv Syst.* 2005;10:229–258.
45. Micera S, Navarro X, Carpaneto J, et al. On the use of longitudinal intrafascicular peripheral interfaces for the control of cybernetic hand prostheses in amputees. *IEEE Trans Neural Syst Rehabil Eng.* 2008;16:453–472.
46. Wark HA, Mathews KS, Normann RA, Fernandez E. Behavioral and cellular consequences of high-electrode count Utah arrays chronically implanted in rat sciatic nerve. *J Neural Eng.* 2014;11:046027.
47. Zheng X, Zhang J, Chen T, Chen Z. Recording and stimulating properties of chronically implanted longitudinal intrafascicular electrodes in peripheral fascicles in an animal model. *Microsurgery* 2008;28:203–209.
48. Lago N, Yoshida K, Koch KP, Navarro X. Assessment of biocompatibility of chronically implanted polyimide and platinum intrafascicular electrodes. *IEEE Trans Biomed Eng.* 2007;54:281–290.
49. Patil AC, Thakor NV. Implantable neurotechnologies: a review of micro- and nanoelectrodes for neural recording. *Med Biol Eng Comput.* 2016;54:23–44.
50. Kubiak CA, Kemp SWP, Cederna PS. Regenerative peripheral nerve interface for management of postamputation neuroma. *JAMA Surg.* 2018;153:681–682.
51. Kubiak CA, Kemp SWP, Cederna PS, Kung TA. Prophylactic regenerative peripheral nerve interfaces to prevent postamputation pain. *Plast Reconstr Surg.* 2019;144:421e–430e.
52. Elsohemy A, Butler R, Bain JR, Fahnestock M. Sensory protection of rat muscle spindles following peripheral nerve injury and reinnervation. *Plast Reconstr Surg.* 2009;124:1860–1868.
53. Banks RW. The innervation of the muscle spindle: a personal history. *J Anat.* 2015;227:115–135.
54. Saal HP, Bensmaia SJ. Biomimetic approaches to bionic touch through a peripheral nerve interface. *Neuropsychologia* 2015;79:344–353.
55. Dhillon GS, Kruger TB, Sandhu JS, Horch KW. Effects of short-term training on sensory and motor function in severed nerves of long-term human amputees. *J Neurophysiol.* 2005;93:2625–2633.
56. Dellon AL, Dellon AL. The proximal inset thenar flap for fingertip reconstruction. *Plast Reconstr Surg.* 1983;72:698–702.
57. Fitoussi F, Ghorbani A, Jehanno P, Frajman JM, Pennecot GF. Thenar flap for severe finger tip injuries in children. *J Hand Surg Br.* 2004;29:108–112.
58. Abraira VE, Ginty DD. The sensory neurons of touch. *Neuron* 2013;79:618–639.
59. Ide C. Regeneration of mouse digital corpuscles. *Am J Anat.* 1982;163:73–85.
60. Koshima I, Moriguchi T, Soeda S. Reinnervation of denervated Pacinian corpuscles: ultrastructural observations in rats following free nerve grafts. *Plast Reconstr Surg.* 1993;92:728–735.
61. Chen YY, McDonald D, Cheng C, Magnowski B, Durand J, Zochodne DW. Axon and Schwann cell partnership during nerve regrowth. *J Neuropathol Exp Neurol.* 2005;64:613–622.
62. Chen Z, Pradhan S, Liu C, Le LQ. Skin-derived precursors as a source of progenitors for cutaneous nerve regeneration. *Stem Cells* 2012;30:2261–2270.
63. Khuong HT, Kumar R, Senjaya F, et al. Skin derived precursor Schwann cells improve behavioral recovery for acute and delayed nerve repair. *Exp Neurol.* 2014;254:168–179.
64. Zhang P, Lu X, Chen J, Chen Z. Schwann cells originating from skin-derived precursors promote peripheral nerve regeneration in rats. *Neural Regen Res.* 2014;9:1696–1702.
65. Ekedahl R, Frank O, Hallin RG. Peripheral afferents with common function cluster in the median nerve and somatotopically innervate the human palm. *Brain Res Bull.* 1997;42:367–376.
66. Wu G, Ekedahl R, Hallin RG. Clustering of slowly adapting type II mechanoreceptors in human peripheral nerve and skin. *Brain* 1998;121:265–279.
67. Wu G, Ekedahl R, Stark B, Carlstedt T, Nilsson B, Hallin RG. Clustering of Pacinian corpuscle afferent fibres in the human median nerve. *Exp Brain Res.* 1999;126:399–409.
68. Koschorke GM, Meyer RA, Tillman DB, Campbell JN. Ectopic excitability of injured nerves in monkey: entrained responses to vibratory stimuli. *J Neurophysiol.* 1991;65:693–701.
69. Michaelis M, Blenk KH, Janig W, Vogel C. Development of spontaneous activity and mechanosensitivity in axotomized afferent nerve fibers during the first hours after nerve transection in rats. *J Neurophysiol.* 1995;74:1020–1027.